

MedChemComm

Accepted Manuscript

This article can be cited before page numbers have been issued, to do this please use: S. K. Bagal, M. Kemp, P. Bungay, T. Hay, Y. Murata, E. Payne, E. Stevens, A. Brown, D. C. Blakemore, M. Corbett, D. Miller, K. Omoto and J. S. Warmus, *Med. Chem. Commun.*, 2016, DOI: 10.1039/C6MD00281A.



This is an *Accepted Manuscript*, which has been through the Royal Society of Chemistry peer review process and has been accepted for publication.

Accepted Manuscripts are published online shortly after acceptance, before technical editing, formatting and proof reading. Using this free service, authors can make their results available to the community, in citable form, before we publish the edited article. We will replace this *Accepted Manuscript* with the edited and formatted *Advance Article* as soon as it is available.

You can find more information about *Accepted Manuscripts* in the [Information for Authors](#).

Please note that technical editing may introduce minor changes to the text and/or graphics, which may alter content. The journal's standard [Terms & Conditions](#) and the [Ethical guidelines](#) still apply. In no event shall the Royal Society of Chemistry be held responsible for any errors or omissions in this *Accepted Manuscript* or any consequences arising from the use of any information it contains.



Discovery and optimisation of potent and highly subtype selective Na_v1.8 inhibitors with reduced cardiovascular liabilities

Received 00th January 20xx,
Accepted 00th January 20xx

DOI: 10.1039/x0xx00000x

www.rsc.org/

Sharan K. Bagal,^{*a} Mark I. Kemp,^b Peter J. Bungay,^c Tanya L. Hay,^d Yoshihisa Murata,^b C. Elizabeth Payne,^e Edward B. Stevens,^e Alan Brown,^a David C. Blakemore,^a Matthew S. Corbett,^f Duncan C. Miller,^b Kiyoyuki Omoto,^a Joseph S. Warmus.^f

Voltage-gated sodium channels, in particular Na_v1.8, can be targeted for the treatment of neuropathic and inflammatory pain. Herein is described the discovery and optimisation of a Na_v1.8 inhibiting phenyl imidazole series that delivers chemical equity that possesses high potency and selectivity and is capable of demonstrating good oral pharmacokinetics.

Introduction

Voltage-gated sodium channels (Na_v) are members of the ion channel family and are composed of a transmembrane α -subunit of approximately 260kDa with associated transmembrane β -subunits of lower molecular weight. The family is comprised of nine members Na_v1.1–Na_v1.9 which can be subdivided into tetrodotoxin-sensitive (TTX-S) and tetrodotoxin-resistant (TTX-R) subtypes. Na_vs play a key role in controlling excitability of neurons by regulating the threshold of firing, underlying the upstroke of the action potential and controlling the duration of interspike interval.¹ Non-selective Na_v blockers (e.g. lamotrigine, lacosamide and mexilitine) have been successfully used in the clinic to treat pathological firing patterns of neurons that occur in a range of conditions such as chronic pain and epilepsy. However, such drugs have a narrow therapeutic window due to inhibition of sodium channels in the heart and throughout the central nervous system. Selective block of Na_v channels as pain targets gained traction with the recognition that some Na_v subtypes showed preferential or exclusive expression in peripheral sensory neurons. A number of studies have implicated Na_v1.3, 1.7, 1.8 and 1.9, which are expressed in dorsal root ganglion (DRG) neurons and trigeminal neurons, in nociceptive processing.^{2,3,4} Na_v1.8 is highly (but not exclusively) expressed in

nociceptors,^{5,6} and its expression and function is modulated by agents that cause pain.^{7,8} Genetic ablation of Na_v1.8 in rodents results in deficits in nociception following inflammation, but not neuropathic pain,^{9,10,11,12} while recent human genetic evidence suggest that gain of function mutations in Na_v1.8 contribute to painful peripheral neuropathy.¹³ A-803467 is a selective Na_v1.8 inhibitor that has been used to demonstrate a link between Na_v1.8 knockdown and inflammatory and neuropathic pain (Figure 1). However, A-803467 exhibits poor oral pharmacokinetics in preclinical species.¹⁴ We recently described the optimisation of Na_v1.8 modulator series to deliver subtype selective, state and use dependent chemical matter. This work culminated in the identification of PF-04531083 and PF-01247324 whereby both compounds were shown to be efficacious in preclinical models of neuropathic and inflammatory pain (Figure 1).¹⁵ The present article discusses the discovery of a novel subtype selective Na_v1.8 series identified via pharmacophore based screening. This series has an improved potency, selectivity and solubility profile when compared with PF-04531083 and PF-01247324.

Results

Discovery and optimisation of lead matter

Structural analysis of existing subtype selective Na_v1.8 inhibitors suggested 5,6- and 6,6- biaryl motifs with at least one hydrogen bond donor (HBD) may have a selective Na_v1.8 inhibition profile (Figure 1). Based on this hypothesis, file screening of 5,6- and 6,6- biaryl motifs residing in rule of five physicochemical space and having ≥ 1 HBD was conducted. Data generated in recombinantly expressed hNa_v1.8/ β 1 (Merck Millipore) led to the identification of oxadiazoles **1a** and **1b** (Scheme 1).

^a Worldwide Medicinal Chemistry, Pfizer Global R&D, The Portway Building, Granta Park, Great Abington, Cambridge, CB21 6GS, UK

^b Worldwide Medicinal Chemistry, Pfizer Global R&D, Sandwich UK

^c Pharmacokinetics, Dynamics & Metabolism, Pfizer Global R&D, The Portway Building, Granta Park, Great Abington, Cambridge, CB21 6GS, UK

^d Pharmacokinetics, Dynamics & Metabolism, Pfizer Global R&D, Sandwich UK

^e Pfizer Global R&D UK, The Portway Building, Granta Park, Cambridge CB21 6GS, UK

^f Pfizer Global R&D, Groton Laboratories, Eastern Point Road, Groton, Connecticut 06340, USA

[†] Corresponding Author Email: sharan.bagal@outlook.com

[‡] The authors declare no competing financial interest.

[†] Electronic Supplementary Information (ESI) available: [details of any supplementary information available should be included here]. See DOI: 10.1039/x0xx00000x

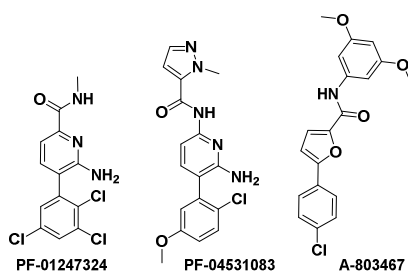
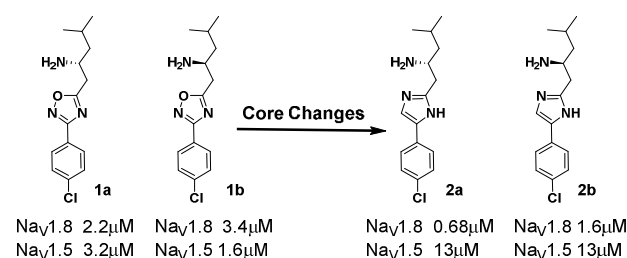


Figure 1. Subtype selective $\text{Na}_v1.8$ inhibitors.^{14,15}



Scheme 1. Phenyl oxadiazole and imidazole $\text{Na}_v1.8$ inhibitors. IC_{50} values were determined at recombinantly expressed $\text{hNa}_v1.8/\beta1$ (Merck Millipore) using manual patch clamp electrophysiology with a conditioning pulse at the $V_{0.5}$ of inactivation. IC_{50} data were generated with at least 2 tests on 2 different assay runs.

Oxadiazoles **1a** and **1b** were low μM inhibitors of $\text{hNa}_v1.8$ but were non-selective over the cardiac ion channel $\text{hNa}_v1.5$. Modification of the oxadiazole core to imidazole improved $\text{hNa}_v1.8$ selectivity over $\text{hNa}_v1.5$ to ~20-fold as exemplified by **2a**. Based on $\text{hNa}_v1.8$ potency and selectivity the phenyl imidazole series was prioritised over the phenyl oxadiazole series. Variation of the chlorophenyl ring of **2a** identified p-CN and p-OCF₃ phenyl as suitable replacements (Figure 2). When compared with **2a** p-CN analogue **3** was weaker at $\text{hNa}_v1.8$ but had a higher LipE whereas the p-OCF₃ derivative **4** was more potent with a lower LipE.

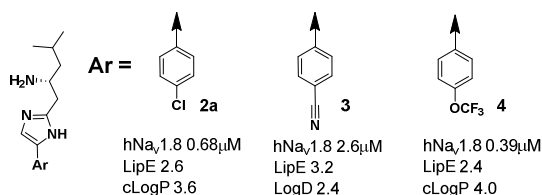


Figure 2. Variation of the phenyl imidazole aryl ring. IC_{50} values were determined at recombinantly expressed $\text{hNa}_v1.8/\beta1$ (Merck Millipore) using manual patch clamp electrophysiology with a conditioning pulse at the $V_{0.5}$ of inactivation. IC_{50} data were generated with at least 2 tests on 2 different assay runs.

At this stage analogue **4** was used as a scaffold to identify the optimal amine fragment expression, the data for which are shown in Table 1. Amines substituted with lipophilic groups e.g. **4-7** and polar substituents e.g. **9-10** were tolerated and increased LipE relative to **4**. There was no significant difference in $\text{hNa}_v1.8$ potency between enantiomers when small lipophilic groups were appended e.g. **2a/b**, **6-7**. Phenyl imidazoles such as **4**, can be synthesised from β -amino acids leading to a 2 carbon spacer between the imidazole and amine (Scheme 2). Synthesis using α -amino acids led to a 1 carbon spacer (Scheme 2). The latter compounds were very potent and LipE efficient e.g. as shown by comparison of **5** and **13**. **13** has a lower cLogP (2.7) and a higher potency ($\text{IC}_{50} = 0.053 \mu\text{M}$) resulting in > 1 unit LipE enhancement when compared with **5**. For a single carbon spacer, if larger lipophilic moieties were appended a 10-fold difference between eutomer and distomer emerged e.g. **11-12**, suggesting that whilst there is a large binding pocket in this region it has size and directionality limitations.

Gem dimethyl derivative **13** was profiled against other sodium channel subtypes in order to assess subtype selectivity (Table 2). Pleasingly, **13** was 80-500-fold selective over the other sodium channel subtypes. However **13** was also active at the human Ether-à-go-go-Related Gene (hERG) ion channel in the patch express (PX) assay ($\text{hERG PX IC}_{50} = 2.6 \mu\text{M}$) leading to a $\text{hNa}_v1.8$ selectivity of ca. 50-fold over hERG. **13** was incubated in human liver microsomes (HLM) and hepatocytes (hHep) in order to understand metabolic liability. Low intrinsic clearance (CL_{int}) was observed (HLM $\text{CL}_{\text{int}} < 8 \text{ uL/min/mg}$, $n = 4$; hHep $\text{CL}_{\text{int}} < 6 \text{ uL/min/million cells}$, $n = 2$) which predicted low metabolic systemic blood clearance (CL) in human (<5ml/min/kg) and corresponding oral bioavailability of >75%. When combined with *in silico* prediction of volume of distribution at steady state (V_{ss}) effective half-life in human was predicted to be ~24 hours.

Optimisation of hERG liability

The profile of compound **13** suggested that the phenyl imidazole series could deliver an acceptable combination of potency, selectivity and pharmacokinetics. However, the hERG selectivity needed improvement with an ideal therapeutic window ≥ 300 -fold.¹⁶ **13** is a basic compound with a measured pKa of 7.9. In order to improve hERG liability a fluorescence polarisation (FP) competition assay was used because it had a higher throughput when compared with the hERG PX assay.¹⁷ The hERG FP assay has been shown to be predictive of compound QT prolongation effects via hERG blockade and can be run in a high throughput 384-well plate manner.¹⁷ In this assay **13** had a hERG FP IC_{50} of 1.8 μM giving an apparent therapeutic index of ~34-fold. There are a number of known methods to reduce hERG liability,¹⁸ one of which is removal of the basic centre. A number of structurally related neutral compounds were prepared **14-17** which reduced the hERG FP potency to an $\text{IC}_{50} > 16 \mu\text{M}$. However there was a concomitant > 20-fold loss in $\text{hNa}_v1.8$ potency ($\text{IC}_{50} > 1 \mu\text{M}$). Another known method to reduce hERG liability is via discrete structural modifications to aryl units which are thought to interact with a

key phenylalanine and/or tyrosine at the hERG ion channel.¹⁸ Modification of the p-OCF₃ phenyl group in **13** to a range of aryl units did indeed reduce the hERG FP potency although there was always an associated loss in hNa_v1.8 potency such that the hERG selectivity did not improve sufficiently. Some representative examples of aryl variations are given in Table 3. If the imidazole core was varied to N-aryl linked imidazole or a triazole there was a substantial reduction in potency in both the hERG FP assay (IC₅₀ >16 μM), and hNa_v1.8 assay (IC₅₀ >1 μM). Based on the SAR generated thus far it appeared that the hNa_v1.8 pharmacophore required the p-OCF₃ aryl unit, imidazole core and basic centre for adequate activity at hNa_v1.8. One region remaining that could be exploited to reduce hERG liability was the gem dimethyl groups. These methyls could be modified to reduce the pKa of the amine in **13** (pKa 7.9), thereby reducing hERG activity. Appending one or two F atoms as in **18** and **19** respectively, reduced the pKa significantly from 7.9 in **13** to 6.4 and 5.9 respectively (Table 1). Gratifyingly, both these fluorinated derivatives were 10-fold weaker at the hERG channel (hERG FP **18** IC₅₀ 14 μM and **19** IC₅₀ 15 μM). However, both these fluorinated derivatives also had > 10-fold reduced activity on hNa_v1.8 leading to weaker compounds with no improvement in hERG therapeutic index. The methyl ether derivative **20** appeared more promising in that this structural change was tolerated by hNa_v1.8 (IC₅₀ = 0.084 μM). **20** was weakly basic at physiological pH having measured pKa 7.1 although the reduction in hERG liability was modest at best (hERG FP IC₅₀ 3.7 μM). Cyclisation of the methyl ether to give an oxetane derivative led to the identification of **21**. This compound retained hNa_v1.8 activity (IC₅₀ 0.047 μM), and had a measured pKa 6.4 which led to a hERG FP IC₅₀ 14 μM and an apparent therapeutic index of ~300-fold. Moreover, **21** was moderately lipophilic (cLogP 2.3) resulting in a respectable LipE of 5. The selectivity and LipE parameters of **21** were noteworthy improvements when compared with **13** (apparent hERG FP therapeutic index 34-fold, cLogP 2.7, LipE 4.6). Oxetane derivative **21** was profiled against the other sodium channel subtypes along with hERG PX in order to assess selectivity (Table 2). Pleasingly, **21** was ca. 350-fold selective over the other sodium channel subtypes and ca. 200-fold selective over the hERG channel (hERG PX IC₅₀ 10 μM). **21** was screened against additional ion channels including KCNQ1, GABA, Ca_v1.2 and Ca_v3.2 where it exhibited minimal activity (% inhibition < 40% at 10 μM). Pharmacokinetic (PK) studies in rat with **21** demonstrated low blood CL (~5ml/min/kg) with oral bioavailability of 49-52% (n = 2).

Docking simulation analysis

Docking simulation analysis was applied in order to understand the hNa_v1.8 protein-ligand interaction mode. As far as we are aware, there are three binding sites for small molecule sodium channel inhibitors, the pore cavity,¹⁹ the voltage-sensor domain,²⁰ and the fenestration site.²¹ Docking analysis was applied to all of the three binding sites, however only docking poses of the fenestration site showed consistency. Docking poses of the other two binding sites were diverse and no

unique binding mode was identified (data not shown). This suggested that the phenyl imidazole compounds described in this work are bound to the fenestration site. Interestingly, the fenestration site has been suggested to be a hNa_v1.8 inhibitor binding site in the literature. Browne et al. reported that site-directed mutagenesis of F1710, which constitutes the fenestration site, to an alanine residue decreased the dissociation constants of Tetracaine and A-803467 with hNa_v1.8 by 3- and 6- fold, respectively.²² The F1710 residue is conserved across all mammalian sodium channel subtypes and a significant drop in affinity or activity of sodium channel inhibitors, such as Etidocaine,²³ Lidocaine,²⁴ and Tetracaine,²⁵ by mutation of this residue has been reported in several publications. Wallace et al. have recently published the X-ray co-crystal structure of a hNa_v1.8 inhibitor PI1 with the NavMS bacterial sodium channel which suggested that PI1 is bound to the fenestration site.²¹ PI1 has the phenyl imidazole scaffold with significant structural similarity to the ligands described in this manuscript, supporting the binding site hypothesis made from the docking simulations.

A potential binding mode for **13** in hNa_v1.8 is illustrated in Figure 3. The binding site extends from the fenestration site to the p-loop and the selectivity filter. Backbone carbonyl oxygen atoms in the selectivity filter from Glu355, Thr1659 and Thr1365 form hydrogen bonds with the protonated amine in the R1 fragment and the imidazole NH and this might contribute to the significant activity of **13** (hNa_v1.8 IC₅₀ 0.053 μM). Similar hydrogen bonds with the p-loop or selectivity filter have been reported for interactions of inhibitors with other voltage-gated ion channels (K_v, Na_v, and Ca_v).²⁶⁻³⁴ This docking model was also consistent with the lower activity of **14** (hNa_v1.8 IC₅₀ > 1 μM) that lacks the hydrogen bond donor in R1. There are very few hydrophobic residues around the selectivity filter and the t-Bu group in R1 is unable to make an effective interaction with the protein. The lower activity of alcohol **15** (hNa_v1.8 IC₅₀ > 1 μM) can probably be explained by the alcohol being a weaker hydrogen bond donor when compared with protonated amines. There are other unsatisfied hydrogen bond acceptors in the selectivity filter (for example, backbone carbonyls of Cys847 and Gly848) and this may have allowed the moderate structural changes in R1 such as carbon insertion or cyclization without a significant change in hNa_v1.8 IC₅₀. Such modifications would alter the orientations and positions of the R1 amines and weaken the original hydrogen bond interactions of **13**, but can create new interactions with other hydrogen bond acceptors in the selectivity filter. The p-OCF₃ aryl unit of **13** was positioned in the centre of the fenestration site which was formed by four residues (L1361, T1365, I1706, and F1710), with a significant π-π stacking interaction with F1710 and van der Waals interactions with L1361, T1365 and I1706. Similar models have been proposed by Tikhonov et al. for the interaction between Tetracaine and hNav1.4.³⁵ In their docking model, the phenyl core of Tetracaine made hydrophobic interactions with F1586, (equivalent to F1710 of Na_v1.8).

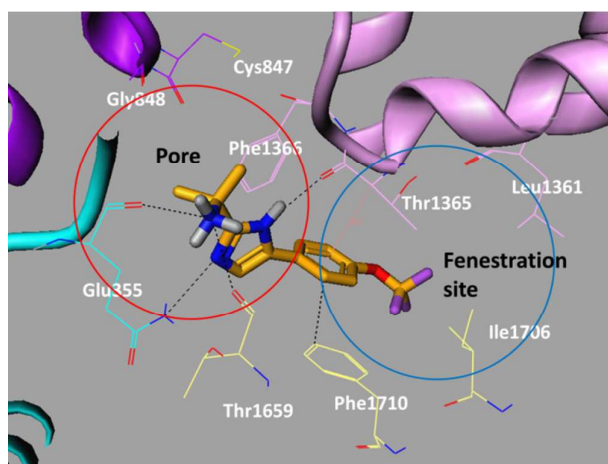
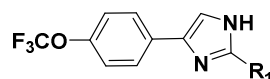


Figure 3. Docking pose of **13** in a human Na_v1.8 homology model. The four domains, D1, D2, D3, and D4 are coloured blue, purple, pink, and yellow, respectively.

Compounds **13** and **21** exhibited species based differential activity at Na_v1.8. **13** and **21** did not inhibit native TTX-R currents in rodent DRG neurons at 10 μM (mouse and rat), but did inhibit native TTX-R currents in cynomolgus monkey DRG neurons at 10 μM (Table 2). The lack of Na_v1.8 activity in rodent precluded preclinical in vivo efficacy studies in these species. Based on the favourable Na_v1.8 potency, LipE, selectivity, in vivo PK, and in vitro cardiovascular risk profile oxetane derivative **21** was selected as a pre-candidate for further progression.

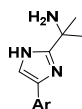


Cmpd	R1	hNa _v 1.8 IC ₅₀ (μM)	cLogP	LipE	Cmpd	R1	hNa _v 1.8 IC ₅₀ (μM)	cLogP	LipE
4		0.39	4.0	2.4	13		0.053	2.7	4.6
5		0.23	3.1	3.5	14		>1	4.8	NA
6		0.32	2.6	3.9	15		>1	2.9	NA
7		0.26	2.6	4.0	16		>1	2.7	NA
8		0.62	3.3	2.9	17		>1	2.5	NA
9		1.6	0.7	5.1	18		0.79	2.6	3.5
10		3.2	1.6	3.9	19		>1	2.3	NA
11		0.036	3.8	3.6	20		0.084	2.4	4.7
12		0.34	3.8	2.7	21		0.047	2.3	5.0

Table 1. Amine fragment SAR observed in the phenyl imidazole series. IC₅₀ values were determined at recombinantly expressed hNa_v1.8/β1 (Merck Millipore) using manual patch clamp electrophysiology with a conditioning pulse at the V_{0.5} of inactivation. IC₅₀ data were generated with at least 2 tests on 2 different assay runs. cLogP was calculated using BioByte program version 4.3.

Cmpd	hNa _v 1.8 IC ₅₀	hNa _v subtype selectivity	TTX-R Rat DRG IC ₅₀	TTX-R Cyno DRG IC ₅₀	hERG PX IC ₅₀
13	0.053 μM	Na _v 1.1 11 μM Na _v 1.2 16 μM Na _v 1.5 27 μM Na _v 1.6 4.2 μM Na _v 1.7 7.0 μM	>10 μM	0.132 μM	2.6 μM
21	0.047 μM	Na _v 1.1 43 μM Na _v 1.2 17 μM Na _v 1.5 36 μM Na _v 1.6 46 μM Na _v 1.7 24 μM	>10 μM	0.070 μM	10 μM

Table 2. hNa_v1.8 potency (IC₅₀) and selectivity (IC₅₀) for **13** and **21**. IC₅₀ values for **13** and **21** at recombinantly expressed hNa_v1.8 /β1 (Merck Millipore) and at TTX-R in rat and cynomolgous monkey (Cyno) DRG were determined using manual patch clamp electrophysiology. hNav subtype selectivity for **13** and **21** was measured using manual patch clamp (Na_v1.1, Na_v1.2, Na_v1.6 and Na_v1.8) or PatchXpress (Na_v1.5 and Na_v1.7) electrophysiology. IC₅₀ values determined using patch clamp electrophysiology were determined at the respective V_{0.5} of inactivation for TTX-R and each channel isoform. IC₅₀ data were generated with at least 2 tests on 2 different assay runs.

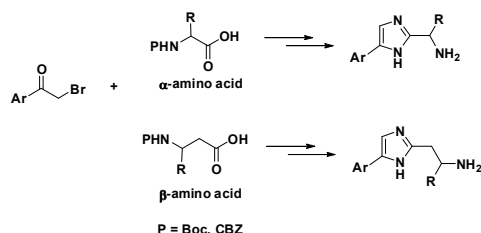


Cmpd	Ar	hNa _v 1.8 IC ₅₀ (μM)	cLogP	hERG FP IC ₅₀ (μM)	hERG FP / hNa _v 1.8
13	4-(trifluoromethoxy)phenyl	0.053	2.9	1.8	34
22	Phenyl	> 1.0	1.7	> 16	-
23	4-chlorophenyl	0.71	2.5	> 16	> 23
24	4-(methylsulfonyl)phenyl	> 1.0	0.1	> 16	-
25	3-(trifluoromethoxy)phenyl	2.2	2.9	9.0	4
26	4-methoxyphenyl	1.0	1.8	> 16	> 16

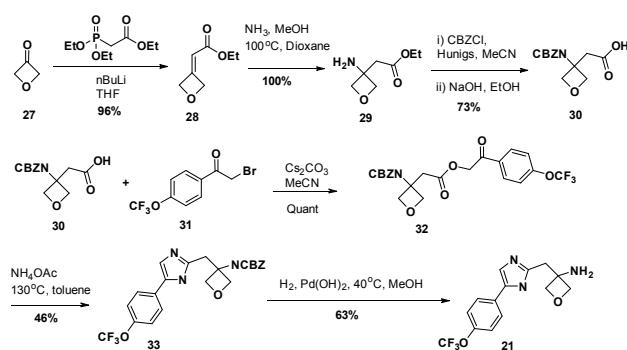
Table 3. Aryl unit SAR observed in the phenyl imidazole series. IC₅₀ values were determined at recombinantly expressed hNa_v1.8/β1 (Merck Millipore) using manual patch clamp electrophysiology with a conditioning pulse at the V_{0.5} of inactivation. IC₅₀ data were generated with at least 2 tests on 2 different assay runs. cLogP was calculated using BioByte program version 4.3. hERG measured using a fluorescence polarisation assay using a Cy3B tagged ligand that binds to the hERG product expressed in HEK-293S cells.³⁶

Synthesis

Scheme 2 demonstrates a general conversion of α - and β -amino acids to give phenyl imidazoles with a 1 or 2 carbon spacer between the imidazole and amine respectively. In this sequence, a bromoketone is reacted with the carboxylic acid of the amino acid to form a ketoester that is cyclised with ammonium acetate in toluene (or xylene) at reflux.^{37, 38} The amino group of the amino acid is protected with a tert-butyloxycarbonyl (Boc) or carboxybenzyl (CBZ) group in this reaction. This cyclisation approach proved both broad in scope and straightforward to carry out and its use is illustrated in the synthesis of analogue **21** as shown in Scheme 3. Starting from oxetan-3-one, Horner-Wadsworth-Emmons reaction gave the enoate **28**. Subsequent reaction with ammonia in methanol gave the beta-amino acid **29**. CBZ protection of the amine was followed by ester hydrolysis to give amino acid **30**. This was reacted with bromoketone **31** to give the cyclisation precursor, **32**. Ketoester **32** was refluxed with ammonium acetate in toluene forming the desired imidazole **33**. Deprotection of the CBZ protected amine gave the desired product **21**.



Scheme 2. General preparation of phenyl imidazoles where Ar=Aryl group



Scheme 3. Preparation of compound **21**.

Conclusions

In conclusion, optimisation of an oxadiazole lead has delivered a highly selective $\text{Na}_v1.8$ series. Compound **13** demonstrated

good potency, excellent subtype selectivity and in vivo PK but suffered from an insufficient therapeutic index over the hERG ion channel. Through a combination of reducing amine pKa, sterically hindering the amine and introducing cyclic conformational restraints, an acceptable potency and selectivity profile was achieved with oxetane derivative **21**. Oxetane **21** was progressed to preclinical toxicology studies and further development data will be reported in due course.

Notes

All studies with animals were conducted in compliance with appropriate national regulations and subject to review by the Pfizer Animal Ethics Committee which includes external members.

Abbreviations

Boc, tert-butyloxycarbonyl; Cmpd, compound; CBZ, Carboxybenzyl; hERG, human Ether-à-go-go-Related Gene product; hERG PX, hERG patch express assay; hERG FP, hERG fluorescence polarisation assay; CL, Clearance; DRG, dorsal root ganglion neuron; HBD, hydrogen bond donor; i.v., intravenous; L/Kg, litres per kilogram; $\mu\text{g}/\text{mL}$, microgram per millilitre; PK, Pharmacokinetics; TTX-S, tetrodotoxin-sensitive; TTX-R, tetrodotoxin-resistant. LipE, lipophilic efficiency; p.o. pharmacokinetic study with oral administration.

References

- Lampert AE, Mirjam; Waxman, Stephen G. . *Handbook of experimental pharmacology*. 2014, **221**, 91.
- Dib-Hajj SD, Cummins TR, Black JA, Waxman SG. *Annu Rev Neurosci*. 2010, **33**, 325.
- Zhang XY, Wen J, Yang W, Wang C, Gao L, Zheng LH, et al. *Am J Hum Genet*. 2013, **93**, 957.
- Leipold E, Liebmann L, Korenke GC, Heinrich T, Giesselmann S, Baets J, et al. *Nat Genet*. 2013, **45**, 1399.
- Amaya F, Decosterd I, Samad TA, Plumpton C, Tate S, Mannion RJ, et al. *Mol Cell Neurosci*. 2000, **15**, 331.
- Shields SD, Ahn H-S, Yang Y, Han C, Seal RP, Wood JN, et al. *Pain*. 2012, **153**, 2017.
- England S, Bevan S, Docherty RJ. *J Physiol* 1996, **495**, 429.
- Dib-Hajj SD, Fjell J, Cummins TR, Zheng Z, Fried K, LaMotte R, et al. *Pain*. 1999, **83**, 591.
- Akopian AN, Souslova V, England S, Okuse K, Ogata N, Ure J, et al. *Nat Neurosci*. 1999, **2**, 541.
- Kerr BJ, Souslova V, McMahon SB, Wood JN. *NeuroReport*. 2001, **12**, 3077.
- Minett MS, Falk S, Santana-Varela S, Bogdanov YD, Nassar MA, Heegaard A-M, et al. *Cell Rep*. 2014, **6**, 301.
- Nassar MA, Levato A, Stirling LC, Wood JN. *Mol Pain*. 2005, **1**, 24.
- Faber CG, Lauria G, Merckies ISJ, Cheng X, Han C, Ahn H-S, et al. *Proc Natl Acad Sci U S A*. 2012, **109**, 19444.

ARTICLE

Journal Name

14. Jarvis MF, Honore P, Shieh C-C, Chapman M, Joshi S, Zhang X-F, et al. *Proc Natl Acad Sci U S A*. 2007, **104**, 8520.
15. Bagal SK, Bungay PJ, Denton SM, Gibson KR, Glossop MS, Hay TL, et al. *ACS Medicinal Chemistry Letters*. 2015, **6**, 650.
16. Meanwell NA. *Tactics in Contemporary Drug Design*: Springer Berlin Heidelberg; 2014.
17. Deacon M, Singleton D, Szalkai N, Pasieczny R, Peacock C, Price D, et al. *Journal of Pharmacological and Toxicological Methods*. 2007, **55**, 255.
18. Jamieson C, Moir EM, Rankovic Z, Wishart G. *J Med Chem*. 2006, **49**, 5029.
19. Bruhova I, Tikhonov DB, Zhorov BS. *Mol Pharmacol*. 2008, **74**, 1033.
20. McCormack K, Santos S, Chapman ML, Krafte DS, Marron BE, West CW, et al. *Proc Natl Acad Sci U S A*. 2013, **110**, E2724.
21. Bagneris C, DeCaen PG, Naylor CE, Pryde DC, Nobeli I, Clapham DE, et al. *Proc Natl Acad Sci U S A*. 2014, **111**, 8428.
22. Browne LE, Blaney FE, Yusaf SP, Clare JJ, Wray D. *J Biol Chem*. 2009, **284**, 10523.
23. Ragsdale DS, McPhee JC, Scheuer T, Catterall WA. *Science*. 1994, **265**, 1724.
24. Ragsdale DS, McPhee JC, Scheuer T, Catterall WA. *Proc Natl Acad Sci U S A*. 1996, **93**, 9270.
25. Li HL, Galue A, Meadows L, Ragsdale DS. *Mol Pharmacol*. 1999, **55**, 134.
26. Ander M, Luzhkov VB, Aqvist J. *Biophys J*. 2008, **94**, 820.
27. Bergson P, Lipkind G, Lee SP, Duban ME, Hanck DA. *Mol Pharmacol*. 2011, **79**, 411.
28. Caballero R, Moreno I, Gonzalez T, Valenzuela C, Tamargo J, Delpon E. *Cardiovasc Res*. 2002, **56**, 104.
29. Decher N, Kumar P, Gonzalez T, Pirard B, Sanguinetti MC. *Mol Pharmacol*. 2006, **70**, 1204.
30. Franqueza L, Longobardo M, Vicente J, Delpon E, Tamkun MM, Tamargo J, et al. *Circ Res*. 1997, **81**, 1053.
31. Lipkind GM, Fozzard HA. *Mol Pharmacol*. 2010, **78**, 631.
32. Snyders DJ, Yeola SW. *Circ Res*. 1995, **77**, 575.
33. Snyders J, Knoth KM, Roberds SL, Tamkun MM. *Mol Pharmacol*. 1992, **41**, 322.
34. Yeola SW, Rich TC, Uebele VN, Tamkun MM, Snyders DJ. *Circ Res*. 1996, **78**, 1105.
35. Tikhonov DB, Zhorov BS. *Mol Pharmacol*. 2012, **82**, 97.
36. Deacon M, Singleton D, Szalkai N, Pasieczny R, Peacock C, Price D, et al. *J Pharmacol Toxicol Methods*. 2007, **55**, 238.
37. Davidson D, Weiss M, Jelling M. *The Journal of Organic Chemistry*. 1937, **02**, 328.
38. Strzybny PPE, Es Tv, Backeberg OG. *The Journal of Organic Chemistry*. 1963, **28**, 3381.

